Energy & Buildings 203 (2019) 109454

Contents lists available at ScienceDirect

Energy & Buildings

journal homepage: www.elsevier.com/locate/enbuild

Evaluation of climate-based daylighting techniques for complex fenestration and shading systems

E. Brembilla[a,*], D.A. Chi[b], C.J. Hopfe[a], J. Mardaljevic[a]

[a] School of Architecture, Building and Civil Engineering, Loughborough University, Loughborough, Leicestershire LE11 3TU, UK
[b] Department of Architecture, Universidad de las Americas Puebla, San Andres Cholula, Mexico

ARTICLE INFO

Article history:
Received 6 June 2019
Revised 7 August 2019
Accepted 22 September 2019
Available online 23 September 2019

Keywords:
Complex Fenestration Systems (CFS)
Climate-Based Daylight Modelling (CBDM)
Radiance
BSDF
Solar energy
Facades

ABSTRACT

The latest advancements in glazing technology are driving facade design towards complex and adaptive fenestration systems. Accurate simulation of their optical properties and operational controls for building daylight performance evaluation requires advanced modelling techniques, such as climate-based daylight modelling (CBDM). At the same time, computational efficiency is key to quickly simulate this complex performance over a full year. Over the years, several CBDM techniques were developed to answer these two main challenges, but they were never systematically benchmarked against each other. This paper compares state-of-the-art RADIANCE-based simulation techniques in terms of annual daylight performance metrics required by national guidelines and international green building rating schemes. The comparison is performed on three different shading systems: diffuse Venetian blinds, specular Venetian blinds, and perforated solar screens. Findings show that simulation methods are characterised by significant differences in their implementation and visual rendering, but most annual daylight metrics result in consistent values (within ±20%). A notable exception is Annual Sunlight Exposure, which is highly sensitive to the chosen simulation method, with differences of up to 47 percentage points. Additional outcomes from the present work are used to compile a list of generalised recommendations for designers and policy makers.

1. Introduction

Shading devices have been used for centuries to offer protection from excessive solar radiation. At the same time, they should allow and modulate some daylight access as well as leaving an outside view whenever possible. Nowadays, shading systems have become a critical issue for global energy performance of buildings that should be responsive to variable climatic conditions and to occupant comfort necessities. Influential compliance schemes such as LEED include assessments based on the accurate prediction of sunlight entering the space. Different studies have highlighted the significant effect of shading devices on indoor daylight quality and on energy savings [1,2]. For some shading devices, such as overhangs, fins and awnings, an acceptable analysis can be done using simple calculations. For other devices such as Venetian blinds, louvres, screens and roller shades, a more sophisticated evaluation process is needed due to their complex geometries and optical properties [3]. Often though, simplified models are still being used to study these complex cases, e.g. considering all surfaces as perfect diffuse materials, or modelling solar shading systems as uniform parallel layers which reduce incoming light flux without taking into account components of daylight redirection [4]. These limitations affect the accuracy of complex fenestration systems' evaluations since they do not consider the strong angular dependency of light transmission that can significantly impact the spatial distribution of daylight in a space.

Given the widespread use of complex shading devices and the greater market penetration of yet more complex glazing materials, it is important that evaluations are founded on accurate characterisation of the materials and robust simulation techniques. Performance evaluation of complex shading devices, including daylight redirecting systems, has been reported by number of authors [5,6]. Most evaluations employ the RADIANCE lighting simulation system [7]. This software has been widely applied due to its physically accurate rendering capabilities and the rigorous validation tests that it has been subjected to [8,9]. For more than two decades RADIANCE has been regarded to be the most reliable tool for lighting simulation for buildings.

A high degree of integration of design and research is still required to address limitations associated with incorporating 'performance criteria' for daylight evaluation of spaces with complex shading devices. For a favourable daylighting strategy that helps

* Corresponding author.
E-mail address: e.brembilla@lboro.ac.uk (E. Brembilla).

https://doi.org/10.1016/j.enbuild.2019.109454

reducing energy use, the building's performance should be determined effectively and simulated at the design stage. A variety of methods used for communicating the availability of daylight and the effect of sun shading have been developed [10]. These mainly refer to various 'performance indicators' that quantify the amount of skylight or sunlight that reach indoor spaces. Climate-Based Daylight Modelling (CBDM) provides the framework for a complete, year-round, evaluation of the building's daylit environment [11]. CBDM performance metrics have been defined for space characterisation and included in design guidelines that are actively promoted by government departments [12] and even made mandatory [13]. Thus, building designers turned to simulation as a means of demonstrating compliance with various schemes [14]. This has encouraged the development of a constantly evolving number of software packages that are either dedicated to CBDM or offer it as part of the suite of evaluation tools. DIVA-for-Rhino, OpenStudio and Groundhog are some examples of commonly used packages which are mainly based on the RADIANCE ray-tracing engine [15].

This paper evaluates multiple different RADIANCE-based simulation techniques that are currently used by both researchers and practitioners to assess the daylighting performance of spaces with Complex Fenestration Systems. The evaluation is based on an inter-model comparison that takes the results from the 4-component method as a relative reference to benchmark all other techniques, as done in a previous work that analysed only clear glazing cases [16]. Here, the analyses carried out in a preceding paper [17] were expanded to consider three types of commonly used Complex Fenestration Systems (CFS): diffuse Venetian blinds, specular Venetian blinds, and perforated solar screens.

2. Modelling Complex Fenestration Systems

Complex Fenestration Systems (CFS) refer to all non-specularly transmitting fenestration technology including layers that provide shading and layers that improve interior daylighting [18]. A non-specular transmission occurs when an incident ray is redirected by the CFS. Notwithstanding the fact that the most commonplace CFS (i.e. venetian blinds) has been an intrinsic feature of facade shading systems for more than half a century, the prediction of the light scattering properties of CFS remains an open research field due to the complexities both of the characterisation of the optical properties and their implementation in a lighting simulation program.

Computational methods, tools and supporting data have been developed to accurately describe the optical properties and daylighting performance of CFS [18,19]. Additionally, new CFS modelling capabilities have been added to building simulation programs. One is the Bi-directional Scattering Distribution Function (BSDF), used to characterise the angularly resolved transmission and reflection of light of CFS. LBNL WINDOW implements the Klems' matrix multiplication algorithm to generate BSDF data of multi-layered fenestration system from the angularly resolved data of single layers, which could be independently measured or calculated [20]. It is also possible to generate BSDF data for a CFS using lighting simulation if the light transport through the CFS can be adequately represented in the simulation. For example, RADIANCE includes the tool `genBSDF` to generate BSDF datasets from the geometry of macroscopic systems and surface properties of the base materials [7].

The first RADIANCE-based CBDM technique that allowed the insertion of BSDF materials to describe CFS was the 3-phase method. Based on the Daylight Coefficient approach, it separates the light transport between the outdoor and the indoor environments into three phases: exterior transport (Daylight matrix, **D**); fenestration transmission (Transmission matrix, **T**) through a BSDF dataset generated on a Klems basis of 145 × 145 bins; and interior transport (View matrix, **V**) [7,21]. This method was mainly introduced for concept design stage and for parametric analyses, as the Klems basis leads to an averaging of the incident light over large solid angles, making it unsuitable for precise representation of light peaks transmission.

The 5-phase method was later introduced as an alternative to enable simulations of CFS at a higher accuracy. The 5-phase method takes the results from the three phase method, then it subtracts the direct sunlight component and recalculates it in a more accurate way by using 5185 sun-like sources evenly distributed on the sky vault and by using variable-resolution Tensor Tree BSDF material instead of the Klems one. In this way, it is a more accurate solution for specular or semi-specular systems [22]. The 4-phase and 6-phase methods were later added to the suite of 'phased' method to allow for the simulation of non-coplanar CFS [23].

Other RADIANCE-based methods preceded the two already presented. The 4-component method, DAYSIM and the 2-phase method were the first examples of annual daylight simulation tools that also took advantage of the Daylight Coefficient approach. Although they were not specifically developed to handle complex fenestration systems, they are included in this work as they are widely used to assess the luminous performance of building spaces, including those with CFS.

The 4-component method calculates the contribution of each of the following daylight components: direct sunlight, indirect sunlight, direct skylight and indirect skylight. The indirect components are obtained using RADIANCE stochastic sampling, with a Tregenza sky division [24] formed by 145 circular patches for indirect sunlight and 145 rectangular patches for indirect skylight. The direct sunlight is obtained from a deterministic way, where the sun is represented by 2056 (or 5035 if a finer description is needed) fixed points evenly distributed on the sky vault. The direct skylight component is also obtained deterministically, as 900 light point sources are placed over each of the 145 rectangular patches covering the whole hemisphere [11]. The 4-component method is used as a benchmark in many studies because it is widely regarded as the most rigorously validated (for clear glazing) of all the various CBDM techniques [25].

DAYSIM is one of the most widespread tools to perform CBDM, as it is often used as simulation engine by commercial tools with graphic interfaces. In its original version [26], the sky is subdivided in 145 patches for the indirect light component, while for the direct sunlight there are up to 65 representative sun positions, depending on the location. Additionally, there are three concentric circular daylight coefficients for the external ground. Later on, the Dynamic Daylight Simulation (DDS) [27] was proposed, including separate calculations for 145 diffuse sky segments, one diffuse ground segment, 145 indirect solar positions and 2305 direct solar positions evenly distributed around the sky vault. DAYSIM includes three different calculation modes but the widely available version is based on the interpolation algorithm. This mode distributes the luminance from the sun among four solar positions that circumscribe the actual sun at any given time of the year. The luminance distribution is derived from climate data files using the Perez All-Weather model [28].

Finally, the 2-phase method assigns the sun luminance to three sky patches surrounding the actual sun position. The sky subdivision can have variable resolution by subdividing each patch in smaller parts (Multiplication Factor, MF). The sun and sky contributions can therefore be accounted for in a single stochastic sampling run and the computation load can noticeably diminish. However, to prevent sampling errors around the sun region, the ambient interpolation is switched off and the ray-tracing mainly relies on the number of ambient divisions (`-ad`).

To date, there have been some studies which investigated different modelling strategies to represent CFS properties. However,

these models have been focused on prediction of solar gains through CFS in building simulation programs [29–31]. In those works, the shading control strategies were dependant on thermal variables, such as indoor air temperature and energy load. When they had calculated daylight illuminances or solar radiation, they mainly tested one RADIANCE-based method (e.g. the 3-phase method) against EnergyPlus. To date, no studies have systematically compared multiple RADIANCE-based approaches to model spaces with CFS. Consequently, practitioners who are increasingly relying on lighting simulation tools to demonstrate compliance are lacking the necessary guidance to help them select the appropriate CBDM methodology for designs which include CFS. The study described here aims to address this deficiency.

3. Methodology

To evaluate the options available when modelling CFS with RADIANCE-based methods and to understand how they compare to each other, a case study room was modelled with three different shading systems in place. These three systems were each simulated with five simulation techniques, varying their representation according to the simulation strategy. The following sections describe the characteristics of the case study and the precise procedures followed to run climate-based daylight simulations.

3.1. Description of the case studies

A classroom space with a large South-facing window was chosen as case study. The dimensions of the space are 11.2 m × 7.9 m. It is side-lit from a curtain-wall that occupies a complete side of the room. Table 1 shows the standard reflectances and the visible transmittances applied on the model surfaces. Specularity and roughness were set to be zero where not otherwise specified. Three different shading devices were placed on the glazed facade, as Fig. 1 displays: (1) Diffusing Venetian blinds, (2) Specular Venetian blinds, and (3) Perforated Solar Screen (PSS). These three systems were treated as fixed shadings and applied on the curtain-wall of the room's South facade. Strictly speaking, a thin PSS cannot be classified as CFS as its structure is either blocking light completely or it is letting light through its holes in a 'specular' manner. It was however included in the investigation, as it exemplifies a shading system design obtained through parametric modelling [32]; as some of the investigated simulation techniques were developed with the specific intent of facilitating parametric design, it was deemed significant to include this third shading system in the present analysis.

Table 1
Characteristics of model surfaces.

		Reflectance	
Classroom	Ceiling	0.7	
	Interior walls	0.5	
	Floor	0.2	
	External ground	0.2	
		Reflectance	Specularity
CFS	Diffusing Venetian blinds	0.62	0.0
	Specular Venetian blinds	0.62	0.9
	PSS (Opaque surface)	0.8	0.0
		Visible transmittance	
	Clear windows	0.8	

The first shading device is formed by light diffusing Venetian blinds, placed on the interior side of the glazing, within the depth of the sill. The slats were modelled as simple horizontal surfaces, with zero thickness, 50 mm wide and spaced every 40 mm; their reflectance value was 0.62 and they were treated as perfect diffusers. The second device has the same geometry as the first one, but it was defined as metallic material, with a specularity of 0.90 on both sides of the slats. The third device is a PSS placed outside the room's curtain-wall, 5 mm from it. The PSS was modelled as a three-dimensional solid, measuring 11.5 m width, 3 m height and 3 mm thickness. It has 576 hexagonal holes, equivalent to a 25% perforation ratio. The material assigned to the PSS was characterised by a 0.80 diffuse reflectance.

3.2. Description of CBDM simulation techniques

Five different techniques to perform CBDM were considered for the inter-model comparison: 4-component method (4CM), DAYSIM, 2-phase method (2PH), 3-phase method (3PH), and 5-phase method (5PH). Three different DAYSIM modes were evaluated and three different procedures to implement the 3PH and 5PH methods were also investigated. Table 2 summarizes all included implementations, for each of the three shading system.

To meet the requirements for every simulation method, the 3D model had to be modified. Fig. 2 illustrates the modification applied for each single simulation mode. For the 4CM, DAYSIM and the 2PH methods all the elements of the classroom and of the three shading systems were explicitly modelled. The three DAYSIM cases (B, B1, B2) all used the same geometry, but different daylight simulation methods and release versions. DIVA-for-Grasshopper was the interface used to access the latest available DAYSIM version (v4), which is based on the interpolation mode; DAYSIM v3.1e was accessed through its legacy Java interface, from which the interpolation or DDS options were selected. For the 3PH and 5PH methods, each shading systems required slightly different approaches. Choosing the most appropriate representation of a CFS among the ones described here depends on the accuracy needed and on the availability of BSDF data.

The three procedures for the 3PH method are explained hereafter. For case D1, a 'thick' BSDF was created with `genBSDF`, on a Klems Basis. It sampled the complete curtain-wall system: clear glazing, frames and Venetian blinds. The resulting BSDF is specific to the sampled geometry and its dimensions, and cannot be ap-

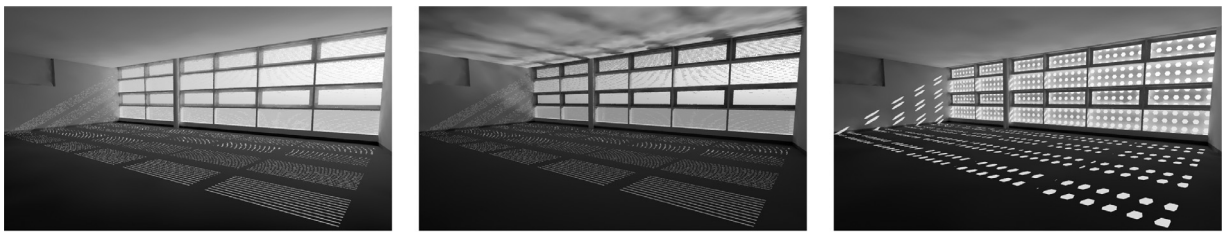

(1) (2) (3)

Fig. 1. Renderings of the classroom from its interior, with each of the three CFS in place: (1) Diffusing Venetian blinds; (2) Specular Venetian blinds; and (3) Perforated Solar Screen.

Table 2
Simulation methods and specific implementations investigated for the comparative analysis of CBDM in the presence of complex fenestration systems.

		Diffusing Venetian blinds	Specular Venetian blinds	PSS
A	4-component method	✓	✓	✓
B	DAYSIM v4 (*DIVA-for-Grasshopper*)	✓	✓	✓
B1	DAYSIM v3.1e *with interpolation mode*	✓	✓	✓
B2	DAYSIM v3.1e *with DDS option*	✓	✓	✓
C	2-phase method	✓	✓	✓
D1	3-phase method *with thick BSDF, from genBSDF*	✓	✓	n/a
D2	3-phase method *with zero thickness BSDF, from genBSDF*	✓	✓	✓
D3	3-phase method *with zero thickness BSDF, from Window6*	✓	n/a	n/a
E1	5-phase method *with thick BSDF, without proxied geometry*	✓	✓	n/a
E2	5-phase method *with thick BSDF, with proxied geometry*	✓	✓	n/a
E3	5-phase method *with zero thickness BSDF*	✓	✓	✓

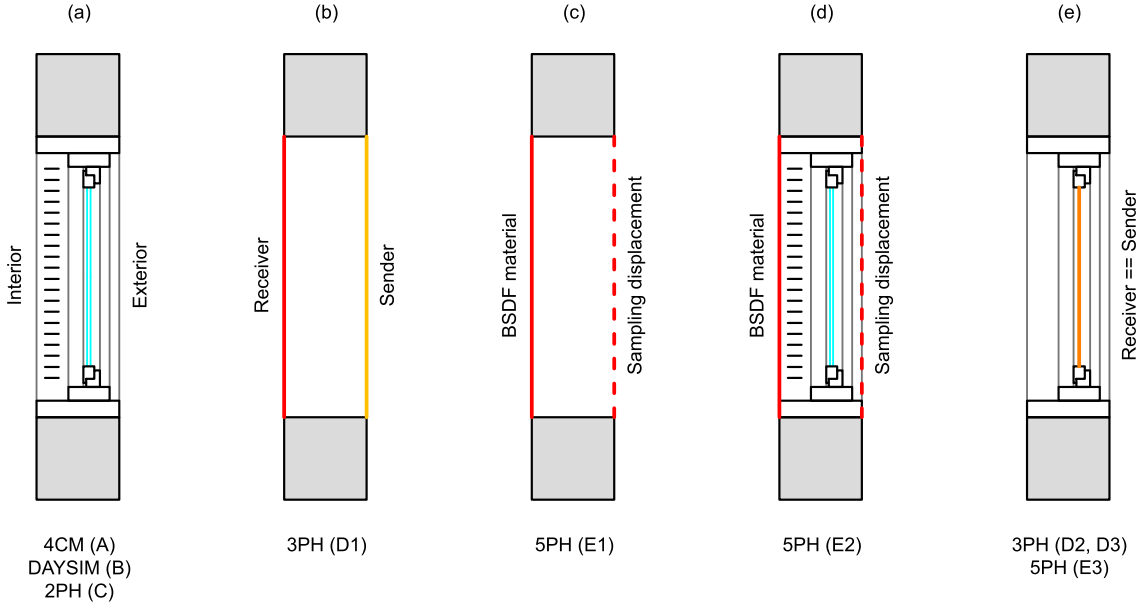

Fig. 2. Schematic illustration of the different modes investigated. Image (a) shows the vertical section of the fenestration system with Venetian blinds on the interior side; for the 4CM, DAYSIM and the 2PH the system was explicitly modelled as shown. Image (b) shows the model modified to be used with the 3PH, where the system was replaced by two enclosing surfaces: a receiver and a sender of rays. The equivalent modification was used for the 5PH – without (c) and with (d) proxied geometry – with a BSDF material representing the whole fenestration system applied to the interior surface and a sampling displacement equivalent to the wall thickness (0.25 m in this case). Lastly, image (e) represents the cases where a 'thin' BSDF was applied, assuming the optical transmission and reflection of both glazing and Venetian blinds happen at the glass surface, which acts as a receiver and a sender of rays.

plied to any generic surface. The 3D model consisted of two surfaces enclosing the wall depth. The surface that faces the interior of the room acts as a receiver for the rays traced from the virtual sensors, while on the exterior side further rays – originated from points randomly distributed over the exterior surface – are sent towards the sky vault. The optical behaviour of the fenestration system enclosed within these two surfaces is represented by this 'thick' BSDF.

In the D2 and D3 cases, a 'thin' BSDF was used to describe the combined system of clear glazing and Venetian blinds, while the frame geometry was explicitly modelled as part of the room's 3D geometry. For the D2 case, the BSDF was created using `genBSDF`, on a Klems basis. The command option `-dim` was inserted to select a limited area to be sampled, representative of the overall behaviour of the material, independently of the geometry size. For the D3 case, the system was modelled using components from the LBNL WINDOW library. This option was investigated only for the diffusing Venetian blinds, as it is not possible to insert specular elements from LBNL WINDOW.

For the 5PH method, three different modes were explored. The cases E1 and E2 used a 'thick' BSDF, similar to that for the D1 case but based on the TensorTree scheme. However, when the 5PH method uses a 'thick' BSDF, there is an additional, optional insertion of a *proxied geometry*, i.e. geometry that blocks direct sunlight but is bypassed by off-angle direct-reflected rays. This results in better defined indoor light patterns, as the equivalent of a shadow testing is performed during the sampling. For case E1, a surface was placed on the interior side of the curtain-wall (the same as the internal surface created for the 3PH method in case D1) and the actual fenestration geometry was not modelled. A BSDF material was assigned to that surface, where the BSDF definition was created by using `genBSDF` but specifying the option (-t4 5) for a Tensor Tree basis. For case E2, a proxied geometry for windows and Venetian blinds was included in the model; this required the specification of the system's thickness in the BSDF material definition, so that only direct rays were blocked by the proxied geometry, while off-angle rays bypassed it. Lastly, the E3 case consisted in the generation of a 'thin' BSDF, as done for the D2 case, but using a Tensor Tree basis rather than a Klems one. For more detailed information about the considered methods and the use of BSDFs in these case studies' CFSs, please refer to a more extensive evaluation by Brembilla [33].

Table 3
Radiance ambient parameters set for each method. For the 3PH and 5PH, the different parameter sets refer to the 3PH *view matrix* (vmx), the 3PH *daylight matrix* (dmx), and the 5PH *direct solar contribution* (dsc).

4CM	`-ab 5 -ad 2048 -ar 128 -as 256 -aa 0.2 -lw 5e-3`
DAYSIM v4	`-ab 5 -ad 4096 -ar 512 -as 512 -aa 0.2 -lw 4e-3`
DAYSIM V3.1e	`-ab 3 -ad 4096 -ar 512 -as 512 -aa 0.1 -lw 4e-3`
2PH	`-ab 5 -ad 89600 -lw 1e-5`
3PH (vmx)	`-ab 5 -ad 22400 -lw 5e-5`
3PH (dmx)	`-ab 2 -ad 22400 -lw 5e-5`
5PH (dsc)	`-ab 1 -ad 89600 -lw 1e-5 -dc 1 -dt 0 -dj 1 -st 1 -ss 0`

Thus far, the descriptions of the 3D model mainly explained the Venetian blinds modelling. The number of different simulation cases appropriate for the PSS study was reduced in comparison with all cases considered for the other two shading devices. For instance, the use of a 'thick' system was not deemed necessary for the PSS, which is 3 mm deep and does not produce significant inter-reflections within its depth. In the simulation process required by the 3PH and 5PH methods, a scene where all geometries are assigned a black material is normally used to avoid taking into account any type of specular reflection when calculating the direct illuminance component. Thus, this approach assumes a Lambertian behaviour for all surfaces that are not represented with a BSDF material. As the window panes for this specific model were not part of the fenestration system included in the BSDF, the scripts used to run the analyses had to be modified to exclude the windows from being transformed into black opaque surfaces.

All ambient parameters were set following a convergence test for each of the methods under analysis. The test was based on the agreement of the Total Annual Illumination (TAI) values obtained from multiple simulation runs. TAI is the sum of the illuminance recorded at every hour in a year by each virtual sensor point, also called Annual Light Exposure [34]. It was selected as it was deemed to be more sensitive to changes in parameters than any of the other annual metrics. Table 3 displays the RADIANCE ambient parameters determined for each simulation method when simulating the two Venetian blinds scenarios. In the PSS case slightly different ambient settings had to be specified to reach a satisfactory convergence of TAI results, in particular for the 4CM method, which required the following settings: `-ab 7 -ad 2048 - ar 512 -as 256 -aa 0.15`. The settings used in all DAYSIM-based cases were not increased but they would also have benefited from higher resolution parameters, as results will show later. The 2PH, 3PH and 5PH methods did not need any particular change in ambient parameters. As an approximate indication, the 4CM method took ~10 h to run this simulation, the 2PH method took ~5 h, the 3PH method took about ~1.5 h and the 5PH method took over 10 h, on the same computer.

The weather file used was the EnergyPlus IWEC file for London Gatwick. The occupancy schedule was set to go from 8:00 a.m. to 18:00 p.m. every day of the year, to be similar to the one required by LEED v4. The analysis grid was placed on a horizontal plane 0.80 m above ground level, representing the working plane for typical student activities, such as desk writing and reading. The edge of the workplane was defined at a 0.50 m distance from the room perimeter. The sensor points were arranged in a grid of 0.25 × 0.25 m, except in the case of DAYSIM modes B1 and B2, where the grid had to be coarser (1 m spacing) as a trade-off between accuracy and computation times. The range of metrics employed in this evaluation are listed below.

- Useful Daylight Illuminance (UDI), representing the percentage of the occupied hours where the illuminance level falls into certain ranges [35], and using the later revised ranges [36]: 0–100 lx: UDI-n, or non-sufficient, 100–300 lx: UDI-s, or supplementary, 300–3000 lx: UDI-a, or autonomous, over 3000 lx: UDI-x, or exceeded.
- Daylight Autonomy (DA), representing the percentage of occupied hours where the illuminance level is higher than a set threshold [37], 300 lx in this work. Shading devices operation is not considered here.
- Total Annual Illumination (TAI) results, averaged over the working plane.
- Annual Sunlight Exposure (ASE), which considers only direct sunlight, representing the portion of the working plane where the sensor points recorded illuminances higher than 1000 lx for more than 250 occupied hours [38].

These metrics were chosen as those most commonly found in software with CBDM capabilities and amongst those required in building guidelines, e.g. for the Priority School Building Programme (PSBP) required by the UK Education Funding Agency (EFA) [13]. Metrics which embed algorithms for the control of shading systems were not considered since those algorithms could have masked the differences revealed by the inter-model comparison. Further studies could focus on the impact that the choice of simulation technique has on the modelling of shading operation.

4. Results

The selected annual daylight metrics were used to compare the simulation results for each shading device. The results are presented in the three sections below and the findings drawn from their comparison are presented in the following discussion section.

4.1. Diffusing venetian blinds

For the first analysis – with diffusing Venetian blinds placed in the model – all the possible variations listed in Table 2 were investigated. Fig. 3 shows the annual daylight metrics obtained with each of those simulation technique variants. Except for ASE, all the metrics were found to be in good agreement, with a maximum of four percentage points of difference in the case of UDI and DA, and a maximum relative difference of 18% for TAI calculated with DAYSIM (B1) and with the 5PH (E2). It appears that the slightly lower values achieved by the 4CM and DAYSIM are due to an insufficient sampling of inter-reflected light within the space, and that these two methods would require higher ambient parameter settings to reach the same light levels of the other methods. This partly demonstrates the need for developing specific methods – such as the 3PH and 5PH – to handle CFS more efficiently.

Using the 3PH with a 'thin' BSDF obtained with the `genBSDF` command (D2) or obtained from LBNL WINDOW (D3) did not affect the results of any of the considered metrics. As the Venetian blinds simulated in this case were perfect diffusers of light, the BSDF Klems definition can be reliably obtained from both methods; this finding is in agreement with previous studies that assessed the performance of `genBSDF` [3,18]. The agreement between the BSDF

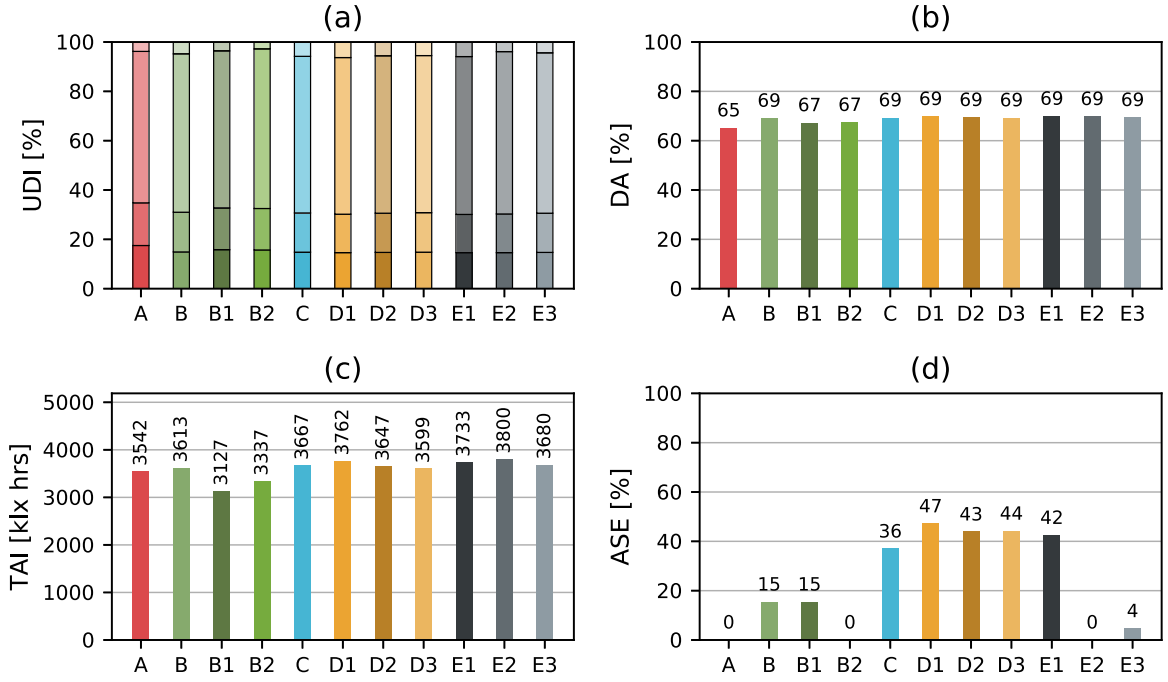

Fig. 3. Annual CBDM metrics for the diffusing Venetian blinds system. The barplot (a) shows the four UDI ranges on the same stacked bar, for all simulation cases; the choice of simulation method did not influenced the final results in terms of UDI. The DA and TAI barplots (b, c) leads to similar conclusions, although it is more noticeable how the 4CM and DAYSIM would benefit of higher ambient parameter settings. The ASE barplot (d) shows the enormous discrepancy in ASE values depending on the simulation method adopted, even though ASE is independent from ambient parameter settings, as it accounts only for direct sunlight.

retrieved from LBNL WINDOW and that created using `genBSDF` further confirms the effectiveness of the simulation approach for certain CFS types.

For ASE, the results are completely independent from the ambient parameter settings since the metric considers only the contribution of direct sunlight onto the workplane (i.e. virtual sensors). Yet, the results are remarkably different among simulation techniques, as visible in Fig. 3(d). The 4CM, DAYSIM (B2) and the 5PH (E2, E3) resulted in very low ($0-4\%$) ASE results; DAYSIM (B, B1) resulted in ASE $= 15\%$; whereas the use of 2PH, all 3PH modes and one 5PH mode (E1) led to ASE values higher than 36%. Note that one of the requirements to achieve a LEED Daylight Credit is an ASE lower than 10%. Thus, the discrepancies revealed here show that compliance outcomes can be significantly affected by the choice of simulation approach – something that many practitioners are probably not aware of.

This discrepancies can be explained by close examination of the direct illuminance values simulated for the whole year by each method. First, from a comparison of the frequency distribution histograms, shown in Fig. 4, and second from plots displaying the instantaneous direct illuminance on the horizontal working plane, shown in Fig. 5 and 6. The histogram shows the frequency distribution of direct illuminance values simulated at each point on the working plane for each hour of the year (1148 points $\times$ 8760 h). The logarithmic scale helps showing the frequency of both low and high illuminance values, even if the latter are much less frequent. The first bin (0–6 klx) includes zero values too, from instances recorded during night-time or from points in the room not directly illuminated by sunlight. Most of the simulation methods produced values within the range 0–12 klx, while a few methods – 4CM (A), DAYSIM (B), 5PH (E2) – recorded instances with direct illuminance over 12 klx, reaching values up to 37 klx with the 5PH (E2). It becomes clearer how this latter group of simulation techniques is able to represent sunlight peaks passing through shading devices, whereas the rest of the methods tend to average them and have a higher frequency of low intensity sunlight instances.

The histograms showed the different distribution of results obtained from an entire year, but from the analysis of point-in-time instances one can discern differences in how the sunlight spatial distribution is computed by each of the methods. Two instances were isolated to show how the illuminance distribution over the working plane changes depending on the chosen method, one from the range 0–6 klx and the other from the range 30–36 klx. The first one is displayed in Fig. 5 and corresponds to the 19th January at 15:00, the second one is displayed in Fig. 6 and corresponds to the 4th March at 12:00. The sensor points recording zero illuminance were set to be coloured white, and the higher values are coloured depending on the logarithmic colour scale displayed on the right of the plots. Under each plot, the following information relative to the selected instant is reported: cumulative illuminance; average illuminance; and number of sensor points recording illuminance higher than 1000 lx (therefore accounted for in ASE calculations).

The simulation methods can be grouped into two types based on their sunlight calculation method: one type can represent well-defined solar patches, whereas the other type ‘smears’ the sunlight over large solid angles, thereby effectively diminishing the magnitude of the predicted component of direct sun. The 4CM employs `rtrace` in its standard mode to predict direct sun. Used in this way, a single shadow ray is sent to test for visibility of the sun, e.g. to determine its illuminance contribution. Although the sun is described as a source solid angle with an opening angle of 0.5°, a single shadow ray is used and so there is no attempt to reproduce the effect of the solar penumbra (which would require multiple shadow ray samples and result in a significant computational overhead). As there is no conceivable practical value to computing the effect of the solar penumbra, this is a perfectly reasonable efficiency saving. Thus, for the computation of direct sun illuminance in the 4CM method, a point is either in sun or in shade based on visibility of the nearest of the 2056 pre-computed direct sun ‘patches’ to the actual sun position at that instant. Consequently, the 4CM results (A) show a distinct sun pattern, created by sunlight rays passing through Venetian blinds and falling onto

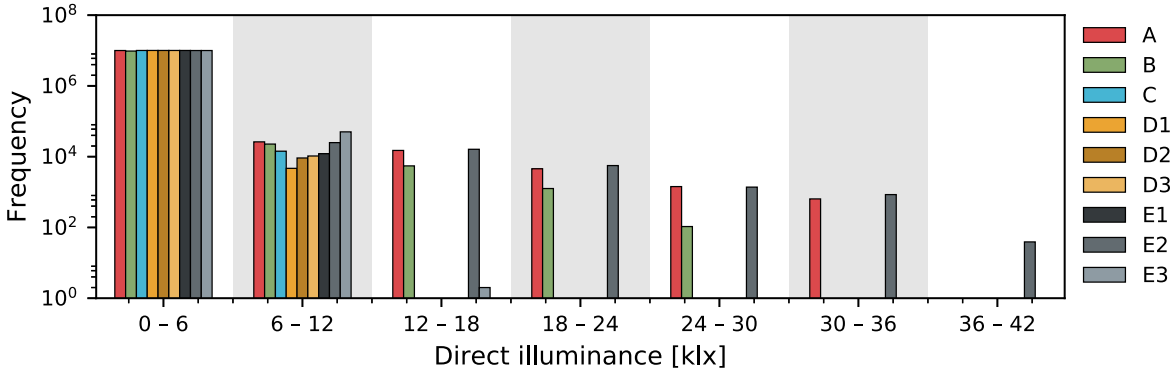

Fig. 4. Frequency distribution of direct illuminance values for each simulation method. Each sample includes direct illuminance values from all sensor points, at every occupied hour in a year. Some of the methods – such as the 4CM (A), DAYSIM (B) and 5PH (E2) – can reach high illuminance peaks over 24 klx, whereas the rest of the methods tend to 'smooth out' any light peak and averaging the overall light intensity over larger areas.

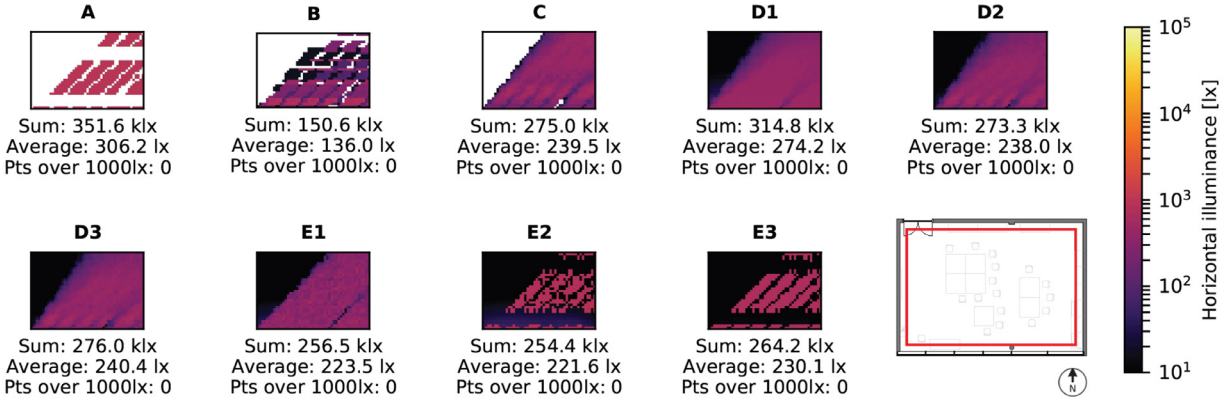

Fig. 5. Direct illuminance distribution over the horizontal working plane (identified by a red line on the room plan view) at 15:00 on 19th January. Depending on the simulation technique, the direct sunlight patterns on the horizontal working plane can look very different: the 4CM (A) and 5PH with proxied geometry (E2) retain the realistic shadow of the CFS; on the opposite hand, all other methods are characterised by an average distribution of direct sunlight that do not preserve information on the CFS geometry. (For interpretation of the references to colour in this figure legend, the reader is referred to the web version of this article.)

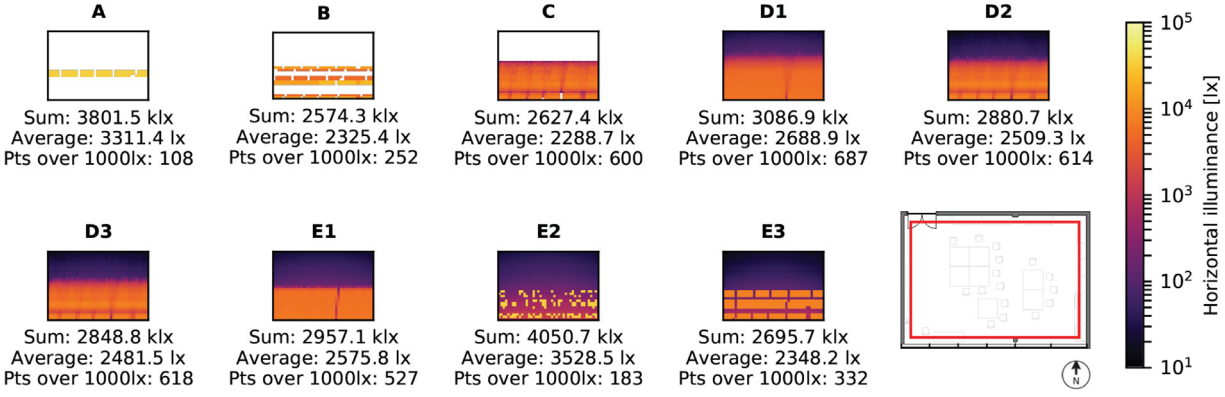

Fig. 6. Direct illuminance distribution over the horizontal working plane (identified by a red line on the room plan view) at 12:00 on 4th March. The differences presented in Fig. 5 can be observed in this Figure too, but here the higher sun angle is partially blocked by Venetian blinds. Hence, in the 4CM plot (A), DAYSIM (B) and 5PH with proxied geometry (E2), only few sensors records high peaks of direct illuminance. As a consequence of this, even though the sunlight intensity is higher than the rest of the methods, there are only a few points hit at each hourly time step, not necessarily reaching the 250 hours (i.e. time steps) necessary to be counted towards ASE. (For interpretation of the references to colour in this figure legend, the reader is referred to the web version of this article.)

the working plane. The low sun angle instance shown in Fig. 5 creates more defined patches as there are more sensors that can 'see' the sun directly, whereas the high sun angle instance of Fig. 6 allows less sensor points to have a direct view of the sun. All sensor points that are not in the sun's direct view record an illuminance value of zero (shaded white in the figure). For the direct sun contribution the 4CM results can be considered benchmark values against which the others are compared.

Although DAYSIM (B) also employs standard `rtrace`, it is configured to compute the weighted contribution from the four (precomputed) suns which are the nearest to the actual sun position at any instant, i.e. the default interpolation mode. This generally

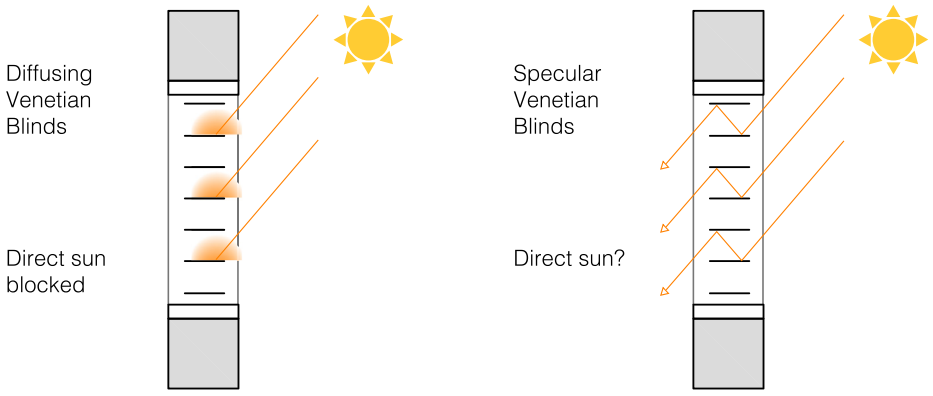

Fig. 7. Schematic visualisation of the difference between transmission of direct sun by diffusing (left) and specular (right) blinds.

results in lower direct sun illuminances than the 4CM, but spread out over a larger area. The pattern resulting from what is effectively multiple suns with different intensities is evident in the Figs. 5 and 6.

The 2PH (C) results in a large illuminance patch falling onto the working plane, in which the shading from the window mullions are barely discernible. With the 3PH (D1, D2, D3) there are no points in the room recording zero illuminance, as even the area at the dark back corner of the room receives some light re-diffused by the BSDF Klems patches. The shadow of the mullions is slightly visible for cases D2 and D3, whereas in case D1 the window frame was not included in the model, and it is therefore not recognisable. The 5PH (E1, E2, E3) creates better defined patches, representing the average light influx in case E1, the actual patches filtering through the windows and through Venetian blinds in case E2 (due to the insertion of *proxied geometry*), or a reduced transmittance window patches in case E3.

Both the 4CM (A) and 5PH (E2) result in higher cumulative and average illuminances than the other methods, as shown in the histogram of Fig. 4. All other cases (B, C, D1, D2, D3, E1, E3) show a remarkable similarity in cumulative and average illuminance values, indicating that the total energy entering the room is about the same but its redistribution in the space is treated differently by each method.

Generally speaking, for evaluations based on average illuminance values, it could be said that the analysed methods are largely interchangeable. However, for direct sun the methods that faithfully reproduce the direct sun component (i.e. 4CM (A), DAYSIM (B2) and 5PH (E2)) all predicted zero ASE values. Whereas, all the other methods – which effectively 'smeared' sunlight over the sensor plane – predicted ASE percentage values ranging between 4 and 47. Thus, depending on the metrics required from the evaluation, the user may need to choose the simulation method very carefully.

4.2. Specular venetian blinds

The use of specular Venetian blinds resulted in higher internal illuminance values compared to the results obtained with diffuse Venetian blinds, due to the more effective transport of light through the blinds by reflection. Consequently, annual metrics such as UDI-a, UDI-x, DA and TAI all reported increased values, irrespective of the simulation method used for the evaluation. The differences among simulation methods, shown in Fig. 8, are larger than for the previous case, but they can be explained by the same reasoning as before. For metrics such as UDI, DA and TAI, the difference is not significant (less than $\pm 20\%$), and it can be largely attributed to the need for higher ambient parameter settings. Whereas for ASE values, the differences are attributable to each method's description of sunlight, as previously explained for the diffusing blinds case.

Recall that ASE is a metric based on direct sun received at the sensor plane. Arrival of sunlight at the sensor plane by specular reflections effectively confounds any assessment based on direct sunlight since its commonplace notion no longer applies, and there is no widely agreed understanding regarding how to classify *redirected* direct sunlight. Furthermore, some materials (both reflecting and transmitting) can have both part-diffusing and part-specular characteristics. For such materials it may be impossible to formulate any rigorous distinction between what constitutes direct sunlight and the other components of illumination. For the study described here, whether or not a ray is considered to be 'direct sun' is more a matter of (largely ad hoc) simulation terminology than agreed upon definitions. This is illustrated in Fig. 7 showing a case where high angle direct sun is completely blocked by the diffusing blinds, but the same geometry for specular blinds could result in the simulation registering the transmission of 'direct sun' rays depending on the technique used. To add to the uncertainty, it is most likely that specular reflection effects did not figure largely (or perhaps at all) in the considerations which ultimately resulted in the formulation of the ASE metric. This should be borne in mind for the evaluation that follows.

For some simulation techniques, the specular Venetian blinds system accentuates the difference with benchmark ASE results even further. Comparing ASE results for the diffuse blinds with those for the specular blinds (Figs. 3(d) and 8(d), it can be noticed that the 2PH (C) result increased of 7 percentage points, and the 5PH (E2, E3) results increased of 18 and 24 percentage points. These increments might be explained by the fact that the 2PH (C) and the 5PH (E2, E3) use one ambient bounce (-ab 1) even for direct sunlight simulations. In the 2PH this bounce is necessary to 'find' the sunlight source, which is represented by sky patches with a `glow` material assigned to them, i.e. the ray-tracing follows a stochastic process rather than a deterministic one. In the 5PH, the extra bounce is necessary to account for off-angle light transmission through a CFS, i.e. the part of sunlight that do not enter the space directly between the blinds slats, but it is reflected off of them and then directed towards the room interior after a single bounce. In effect, if these strong reflections fall within an observer's field of view, the resulting visual discomfort is comparable to those caused by direct sunlight. It is therefore understandable that the recommended 5PH simulation settings are accounting for off-angle transmission effects. It is less clear whether these should be included in the 'direct sunlight' definition that is prescribed in the ASE calculation guidelines. Theoretically, it could be possible to set a zero bounce calculation with the 5PH method – specific for ASE – but at the moment there is not a clear procedure recommending this use of the 5PH. As previously noted, guidelines

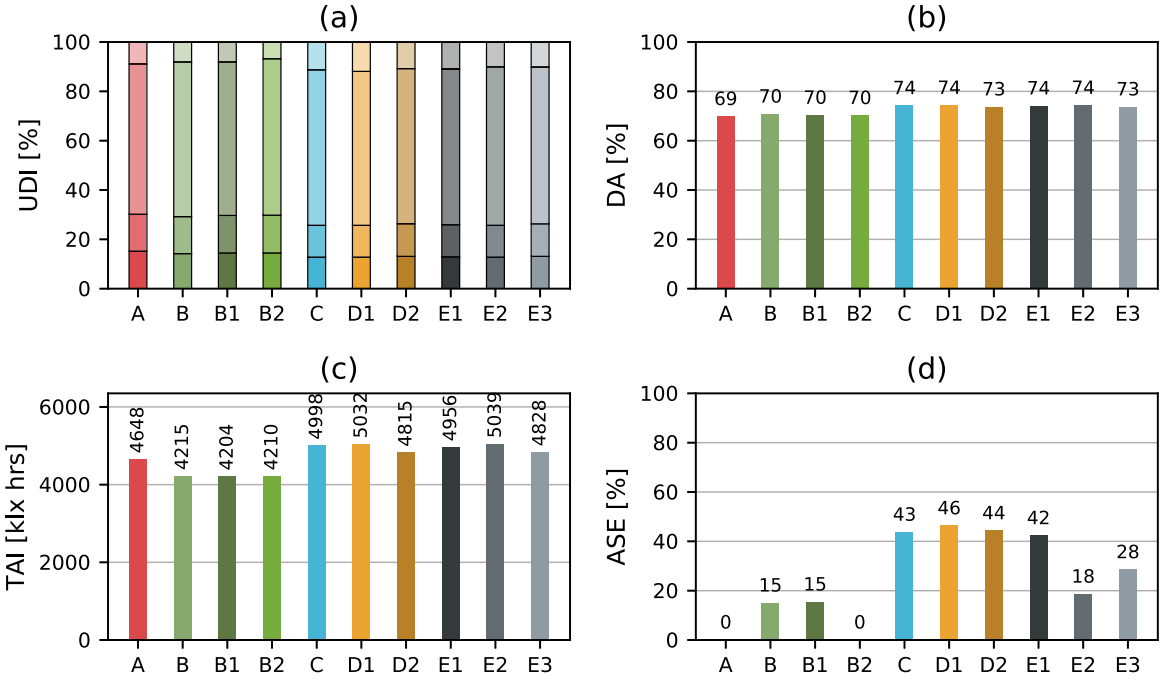

Fig. 8. Annual CBDM metrics for the specular Venetian blinds system. As for the diffusing Venetian blinds system, the barplot (a) shows the four UDI ranges on the same stacked bar, for all simulation cases; the choice of simulation method did not influenced the final results in terms of UDI. The DA and TAI barplots (b, c) leads to similar conclusions, although it is more noticeable how the 4CM and DAYSIM would benefit of higher ambient parameter settings. The ASE barplot (d) shows significant differences among methods, with values of 0% for the 4CM (A) and DAYSIM (B2) and as high as 46% for the 3PH (D1).

defining annual CBDM metrics do not include detailed instructions about specular reflections and about what exactly constitutes direct sunlight.

4.3. Perforated solar screen

The PSS shading system needed to be modelled differently from the other two systems as it was positioned on the exterior side of the fenestration system, hence it was modelled as an independent element. Thus, the BSDF created for the 3PH and 5PH (D2, E3) represented only the PSS – assumed to be a single surface without thickness – while all parts of the windows were explicitly modelled. The number of simulation cases is therefore reduced in comparison with those investigated for Venetian blinds. Even though the PSS is a fixed shading system, the interest in modelling it with a BSDF relies on the possibility of running efficient parametric analyses, say, to find the optimal perforation ratio and shape. For the 4CM, DAYSIM and 2PH, all geometries – windows and PSS – were explicitly modelled.

For methods based on RADIANCE `rtrace`, like 4CM and DAYSIM, PSS were found particularly challenging to simulate, and the time to complete simulation runs was significantly longer than for previous CFS. Fig. 9 shows how an inadequate setting of ambient parameters for DAYSIM (B, B1, B2) influenced all annual CBDM metrics (except for ASE, which does not include ambient light redirection). The 2PH potentially overestimates light levels, as the larger sun angle could be seen through PSS perforations more often than in reality. ASE values for the 2PH and 3PH (C and D2) were surprisingly identical, even if the former accounts for direct sunlight through the actual geometry and the latter accounts for direct sunlight as 'filtered' through the BSDF matrix; ASE for the 5PH (E3) was also found to be similar. However, all of these three methods reported ASE values well higher than the 4CM (A) – which is taken to be the benchmark for ordinary glazing and non-redirecting CFS.

Examining the frequency distribution of direct illuminance shown in Fig. 10, it can be noticed that `rtrace`-based methods, such as 4CM (A) and DAYSIM (B, B1, B2 – but B2 in particular), result in higher direct sunlight values. These peaks are the result of sunlight passing through PSS holes, thus equivalent to a situation where no shading systems are present. For the 3PH (D2) and 5PH (E3), the use of BSDF to represent the PSS leads to the disappearance of any geometrical feature/pattern of the PSS itself (as visible in Fig. 1(c)), and to the averaging of the transmitted light over the whole surface representing the screen. This effect reduces significantly the presence of light peaks in case of the 3PH (D2), which uses BSDF on a Klems basis, and slightly less for the 5PH (E3), which uses a Tensor-Tree basis.

From these results, it would appear that, at present, it is not possible to recommend any simulation technique that is able to reproduce the discontinuous light pattern that the PSS produces within the room and that is computationally efficient for annual evaluations. This is likely to be more critical for glare and visual comfort studies, for which the correct representation – i.e. intensity and directionality – of direct sunlight has a strong impact on the results. For annual metrics that take into account illuminance values averaged on the working plane the choice of simulation technique is less influential, but the correct calibration of RADIANCE parameter settings was found to be essential and particularly challenging for this type of shading geometry.

5. Discussion

The results presented in the previous section show that state-of-the-art CBDM RADIANCE-based methods to simulate CFS are extremely varied in the way they reproduce the effect of direct sunlight onto and through fenestration and shading systems. These differences notwithstanding, some annual CBDM metrics resulted in very similar values, whereas other metrics – such as ASE – are strongly affected by the choice of simulation method. Additionally, methods such as the 3PH or the 5PH offer more than one

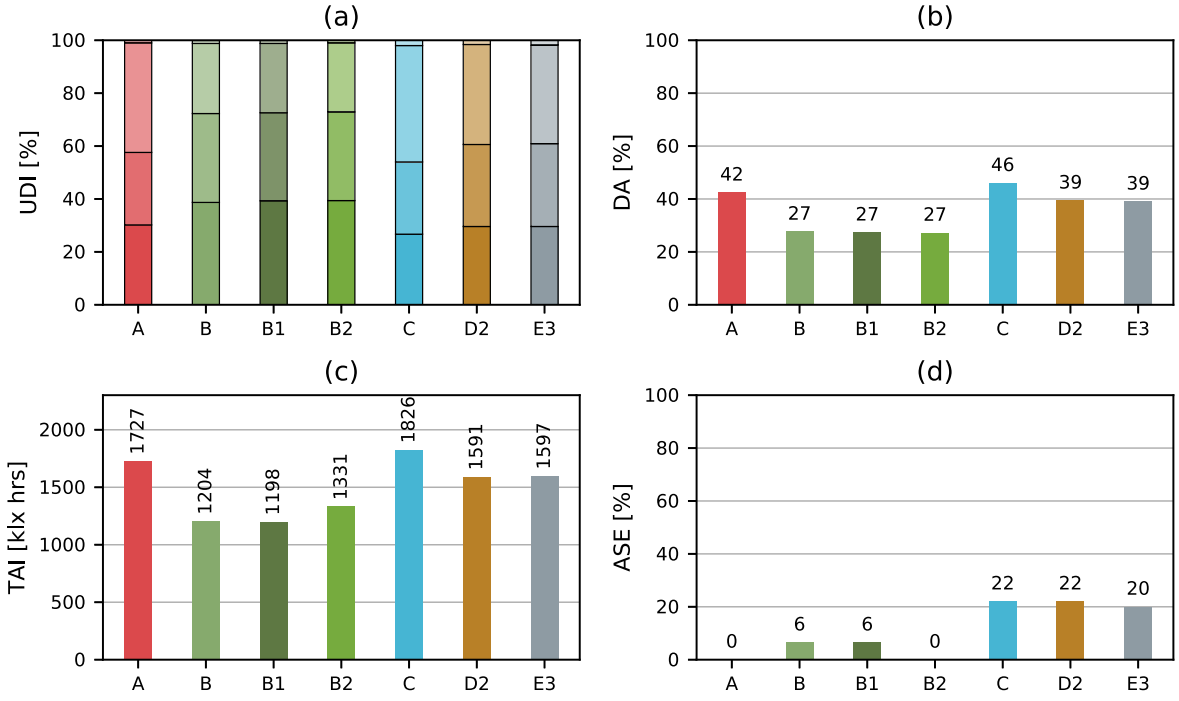

Fig. 9. Annual CBDM metrics for the PSS system. The ambient parameter settings used for the 4CM (A) had to be increased to reach the values shown in the Figure. For DAYSIM (B, B1, B2) the parameter were not increased, thus UDI-a, DA and TAI results are lower than other methods. 2PH (C) resulted in generally higher annual values, likely because the sensors could 'see' the larger sun through the PSS holes more often. 3PH (D2) and 5PH (E3) resulted in very similar values, as both methods represented the PSS as an homogeneous surface with a transmittance proportional to the PSS perforation ratio.

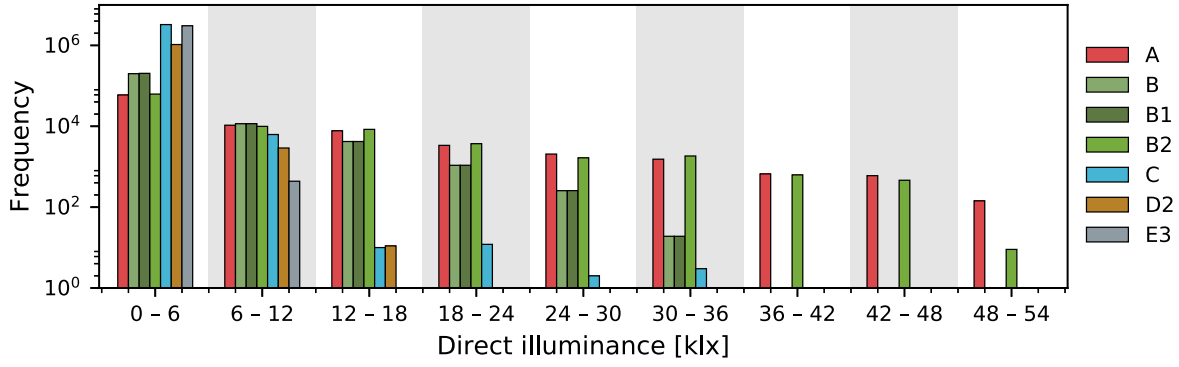

Fig. 10. Frequency distribution of direct illuminance values for each simulation method, when the PSS was applied. Each sample includes direct illuminance values from all sensor points, at every occupied hour in a year. Some of the methods – such as the 4CM (A) and DAYSIM (B2) – can reach high illuminance peaks over 48 klx, whereas the rest of the methods tend to 'smooth out' any light peak and averaging the overall light intensity over larger areas.

approach to solve the same problem, giving the user additional flexibility – and also the potential for making an incorrect choice – when setting up the analysis. Front-end (i.e. user friendly) software tools increasingly offer simplicity in order to lower the 'entry point' skills required to run complex simulations. These tend to offer to the user a single simulation approach wherever possible in order to: (i) reduce software development costs, and (ii) to avoid presenting the (possibly non-expert) user with choices that require an expert's insight in order to make the right/best decision. A single approach could meet the requirements of many users wishing to evaluate only traditional fenestration systems, and depending of which metrics are required. However, for CFS – including commonplace Venetian blinds – a single simulation approach could lead to limitations, which ideally should be made clear in the software specification. In other words, the tool's domain of applicability should be clearly described. An informed user could then select the most appropriate tool for the task, balancing accuracy and simulation speed. For example, a parametric analysis at the concept stage could be performed using the 3PH to run many simulations quickly and still have a reasonable approximation of the prevailing daylight performance. However, when more rigorous evaluations are required and/or if the directionality of light peaks is an important part of the evaluation (e.g. for glare analyses), then the user should consider using other simulation techniques, e.g. 5PH or 4CM (depending on the nature of the CFS), or perhaps also selected point-in-time visualisations with `rtrace`. Guidelines on how to perform CBDM analyses with the RADIANCE phased methods do exist [39], but more accessible information should be also made available to front-end tool users, for them to consciously choose the most appropriate method.

The following considerations are listed with the intent to help designers choosing the most appropriate simulation method for their needs, and to help policy makers taking into account the variability of simulation tools and their implementations when defining performance metrics and targets:

- The use of BSDF materials to describe CFS with macroscopic discontinuities – such as Venetian blinds and PSS – will always result in an averaged homogeneous light transmission within the space, with the complete disappearance of clear sunlight patterns within the space, although in different measure for each simulation method. The 5PH with *proxied geometry* is the only simulation method that makes use of BSDFs and that can closely resemble the effects obtained with `rtrace`.
- The RADIANCE tool `genBSDF` gives the user complete freedom to create BSDF descriptions for any material and system that can be modeled in RADIANCE. For example, as shown in the analysis carried out for this paper, the BSDF can contain only the transmitting part of the fenestration, the whole fenestration system, both fenestration and shading systems, and so forth.
- A CFS composed of microscopic elements or one that completely re-diffuses incoming light can be accurately represented by BSDF created from measurements, whereas CFS composed by macroscopic elements can only be obtained by 'virtually' sampling the modelled geometry with simulation tools such as `genBSDF` [22].
- At the moment of writing, BSDFs retrieved from LBNL WINDOW libraries can only be based on the Klems division, and do not account for specular reflections [18].
- The 2PH and 3PH cannot compute the direct sunlight component by simply setting `-ab 0`; as the sunlight is represented as a `glow` type source, the RADIANCE raytracing process uses a statistical sampling rather than a deterministic one. In order to 'find' the sun, the virtual sensors have to send at least one bounce towards the sky.
- The 5PH uses a `light` source type to represent the sun, and it can therefore account for direct sunlight when setting `-ab 0`. However, as the overall results from the 5PH rely on the diffuse and inter-reflected light calculated with the 3PH, the direct sunlight component obtained with the 5PH has to be consistent with the 3PH direct sunlight component. For this reason, when calculating the 5PH direct sunlight the bounces are set at `-ab 1`, thus accounting for off-angle transmission of direct solar rays due to reflections on the CFS. Guidelines should clearly state whether reflected-direct sunlight should be taken into account or not.

The main limitation in this study is, of course, the absence of a measurement dataset for the various scenarios against which the simulated values could be compared. A truly reliable validation dataset should include measurements of the sky luminance distribution in addition to direct normal illuminance rather than inferring sky conditions from global values [25]. Attempts at validation without sky luminance data can lead to erroneous findings [40]. The long-term measurement of sky luminance patterns has only rarely been carried out, and then usually as part of major studies, e.g. the International Daylight Measurement Programme. Although camera-based capture of sky luminance patterns using high dynamic range imaging may eventually offer an effective replacement for costly sky scanners, these measurements are still some way off from becoming a routine occurrence. All of the simulation methods considered here have undergone some form of validation/testing. However, the validation procedures were different in each case, and each employed differing levels of rigour. Accordingly, for this study the authors have made every effort to make only reasonable extrapolations from existing validation studies when discussing the performance noted here. For example, treating the 4CM prediction of direct sun as a benchmark for the case of diffusing blinds and perforated screen. However it is evident that further research work on the validation of CBDM approaches for CFS should be carried out.

6. Conclusion

This paper has presented and compared state-of-the-art RADIANCE-based techniques to perform Climate-Based Daylight Modelling (CBDM) with facades containing Complex Fenestration Systems (CFS). Three different shading systems were analysed with five CBDM techniques: the 4-component method (4CM); DAYSIM; the 2-phase method (2PH); the 3-phase method (3PH); and the 5-phase method (5PH). For DAYSIM, the 3PH and 5PH methods, multiple implementations and approaches were also considered. The study performed in this paper is the first systematic inter-model comparison to group all these methods.

The analysis focused on the sensitivity of annual daylight metrics to the chosen simulation method. Findings showed that the more traditional methods, i.e. those based on the RADIANCE `rtrace` command – such as the 4CM and DAYSIM – require an increase in ambient parameter settings when CFS are present (e.g. from `-ab 5` to `-ab 7` for the PSS), with consequent increases in computational time. The other methods, based on the `rcontrib` command, are generally more efficient, but at the expenses of a realistic representation of daylight patterns within the room. This is partly due to the use of BSDF representations of CFS, which offers a big potential in terms of computation efficiency, but which can result in averaging and even the disappearance of light peaks. Furthermore, there can be multiple approaches to set up an annual CBDM evaluation with BSDF, even within the same simulation method, e.g. 3PH or 5PH. Guidelines on these different approaches are currently limited, and the choice of an appropriate simulation method depends completely on the user's expertise.

CBDM annual metrics show varying degrees of sensitivity to adopted simulation method. With appropriate ambient parameter settings, metrics based on total illumination – such as UDI, DA and TAI – were found to be comparable across all methods, well within the $\pm 20\%$ uncertainty range expected for daylight simulation. Conversely, ASE values were found to vary significantly depending on the chosen simulation method (up to 47 percentage points), and even when adopting different approaches with the same method (up to 10 percentage points). These findings are in agreement with previous studies that looked at spaces with clear glazing, but this paper shows that when CFS are present, there is an even wider range of possible simulation implementations that can potentially increase the overall uncertainty in annual CBDM results. Guidelines and performance metrics definitions should take this variations into account to avoid misinterpretation. A list of recommendations for designers and policy makers was presented in the discussion section.

This study brought to the attention of the daylight simulation community the vast disparity of tools and implementations that the users are confronted with when evaluating CFS. It is suggested that current guidelines need to take this into account when prescribing performance metrics. To further increase our understanding of the relationship between simulation and reality, future research should also consider how state-of-the-art CBDM techniques relate to data measured in real spaces.

Funding

The research described in this paper was part of Dr Brembilla's PhD 'Applicability of Climate-Based Daylight Modelling'. The PhD was funded by the Engineering and Physical Sciences Research Council and by Arup Lighting UKMEA Group, under the EPSRC CASE Award scheme (Grant EP/K504476/1).

Declaration of Competing Interest

We wish to confirm that there are no known conflicts of interest associated with this publication and there has been no significant financial support for this work that could have influenced its outcome.

Acknowledgements

Dr Brembilla acknowledges the support of the EPSRC and of the industrial partner Arup Ltd. Dr Chi Pool acknowledges the support of IUACC, CONACYT and Erasmus+. Dr Hopfe and Prof Mardaljevic acknowledge the support of Loughborough University.

Supplementary material

Supplementary material associated with this article can be found, in the online version, at doi:10.1016/j.enbuild.2019.109454.

References

[1] W. O'Brien, K. Kapsis, A.K. Athienitis, Manually-operated window shade patterns in office buildings: a critical review, Build. Environ. 60 (2013) 319–338, doi:10.1016/j.buildenv.2012.10.003.
[2] A. Sherif, H. Sabry, T. Rakha, External perforated solar screens for daylighting in residential desert buildings: identification of minimum perforation percentages, Sol. Energy 86 (6) (2012) 1929–1940, doi:10.1016/j.solener.2012.02.029.
[3] G. Molina, Integrated Thermal and Lighting Analysis of Spaces with Controlled Complex Fenestration Systems and Artificial Lighting During the Design Stage, Pontificia Universidad Catolica de Chile, 2014 Ph.D. thesis.
[4] A. GhaffarianHoseini, N.D. Dahlan, U. Berardi, A. GhaffarianHoseini, N. Makaremi, M. GhaffarianHoseini, Sustainable energy performances of green buildings: a review of current theories, implementations and challenges, Renew. Sustain. Energy Rev. 25 (2013) 1–17, doi:10.1016/j.rser.2013.01.010.
[5] G. Molina, W. Bustamante, J. Rao, P. Fazio, S. Vera, Evaluation of radiance's genBSDF capability to assess solar bidirectional properties of complex fenestration systems, J. Build. Perform. Simul. 8 (4) (2015) 216–225, doi:10.1080/19401493.2014.912355.
[6] W. Bustamante, S. Vera, A. Prieto, C. Vásquez, Solar and lighting transmission through complex fenestration systems of office buildings in a warm and dry climate of chile, Sustainability 6 (5) (2014) 2786–2801, doi:10.3390/su6052786.
[7] G. Ward, R.G. Mistrick, E.S. Lee, A. McNeil, J. Jonsson, Simulating the daylight performance of complex fenestration systems using bidirectional scattering distribution functions within radiance, Illum. Eng. Soc. N. Am. 7 (January) (2011).
[8] J. Mardaljevic, Validation of a lighting simulation program under real sky conditions, Light. Res. Technol. 27 (4) (1995) 181–188, doi:10.1177/14771535950270040701.
[9] C. Reinhart, A. Fitz, Findings from a survey on the current use of daylight simulations in building design, Energy Build. 38 (7) (2006) 824–835, doi:10.1016/j.enbuild.2006.03.012.
[10] I.L. Wong, A review of daylighting design and implementation in buildings, Renew. Sustain. Energy Rev. 74 (July 2016) (2017) 959–968, doi:10.1016/j.rser.2017.03.061.
[11] J. Mardaljevic, Daylight Simulation: Validation, Sky Models and Daylight Coefficients, De Montfort University, Leicester, UK, 2000 Ph.D. thesis.
[12] US Green Building Council (USGBC), LEED Reference Guide for Building Design and Construction, LEED V4, Technical Report, USGBC, Washington DC, USA, 2013.
[13] Education Funding Agency, EFA Daylight Design Guide Rev02, Technical Report, Education Funding Agency, London, UK, 2014.
[14] J. Mardaljevic, L. Heschong, E. Lee, Daylight metrics and energy savings, Light. Res. Technol. 41 (3) (2009) 261–283, doi:10.1177/1477153509339703.
[15] N. Jakica, State-of-the-art review of solar design tools and methods for assessing daylighting and solar potential for building-integrated photovoltaics, Renew. Sustain. Energy Rev. 81 (2018) 1296–1328, doi:10.1016/j.rser.2017.05.080.
[16] E. Brembilla, J. Mardaljevic, Climate-Based daylight modelling for compliance verification: benchmarking multiple state-of-the-art methods, Build. Environ. 158 (2019) 151–164, doi:10.1016/j.buildenv.2019.04.051.
[17] E. Brembilla, D.A. Chi Pool, C.J. Hopfe, J. Mardaljevic, Inter-model comparison of five climate-based daylight modelling techniques: redirecting glazing/shading systems, in: Proc. 15th IBPSA Conf., IBPSA, San Francisco, CA, USA, 2017, pp. 1047–1056.
[18] A. McNeil, C. Jonsson, D. Appelfeld, G. Ward, E. Lee, A validation of a ray-tracing tool used to generate bi-directional scattering distribution functions for complex fenestration systems, Sol. Energy 98 (PC) (2013) 404–414, doi:10.1016/j.solener.2013.09.032.
[19] M. Andersen, J. de Boer, Goniophotometry and assessment of bidirectional photometric properties of complex fenestration systems, Energy Build. 38 (7) (2006) 836–848, doi:10.1016/j.enbuild.2006.03.009.
[20] J.H. Klems, A new method for predicting the solar heat gain of complex fenestration systems: II. Detailed description of the matrix layer calculation, in: Am. Soc. Heating, Refrig. Air-Conditioning Eng. Trans., 100, 1994, pp. 1073–1086. New Orleans, LA, USA
[21] A. McNeil, E. Lee, A validation of the radiance three-phase simulation method for modelling annual daylight performance of optically complex fenestration systems, J. Build. Perform. Simul. 6 (1) (2013) 24–37, doi:10.1080/19401493.2012.671852.
[22] E.S. Lee, D. Geisler-Moroder, G. Ward, Modeling the direct sun component in buildings using matrix algebraic approaches: methods and validation, Sol. Energy 160 (September 2017) (2018) 380–395, doi:10.1016/j.solener.2017.12.029.
[23] T. Wang, G. Ward, E.S. Lee, Efficient modeling of optically-complex, non-coplanar exterior shading: validation of matrix algebraic methods, Energy Build. 174 (2018) 464–483, doi:10.1016/j.enbuild.2018.06.022.
[24] P.R. Tregenza, Subdivision of the sky hemisphere for luminance measurements, Light. Res. Technol. 19 (1) (1987) 13–14, doi:10.1177/096032718701900103.
[25] J. Mardaljevic, The BRE-IDMP dataset: a new benchmark for the validation of illuminance prediction techniques, Light. Res. Technol. 33 (2) (2001) 117–134, doi:10.1177/136578280103300209.
[26] C.F. Reinhart, S. Herkel, The simulation of annual daylight illuminance distributions a state-of-the-art comparison of six RADIANCE-based methods, Energy Build. 32 (2) (2000) 167–187, doi:10.1016/S0378-7788(00)00042-6.
[27] D. Bourgeois, C.F. Reinhart, G. Ward, Standard daylight coefficient model for dynamic daylighting simulations, Build. Res. Inf. 36 (1) (2008) 68–82, doi:10.1080/09613210701446325.
[28] R. Perez, R. Seals, J. Michalsky, All-weather model for sky luminance distribution-Preliminary configuration and validation, Sol. Energy 50 (3) (1993) 235–245, doi:10.1016/0038-092X(93)90017-I.
[29] T.E. Kuhn, S. Herkel, F. Frontini, P. Strachan, G. Kokogiannakis, Solar control: a general method for modelling of solar gains through complex facades in building simulation programs, Energy Build. 43 (1) (2011) 19–27, doi:10.1016/j.enbuild.2010.07.015.
[30] J.H. Klems, A new method for predicting the solar heat gain of complex fenestration systems: I. Overview and derivation of the matrix layer calculation, in: Am. Soc. Heating, Refrig. Air- Cond. Eng. Trans., 1994, pp. 1065–1072. New Orleans, LA, USA
[31] B. Bueno, J. Wienold, A. Katsifaraki, T.E. Kuhn, Fener: a radiance-based modelling approach to assess the thermal and daylighting performance of complex fenestration systems in office spaces, Energy Build. 94 (2015) 10–20, doi:10.1016/j.enbuild.2015.02.038.
[32] D.A. Chi, D. Moreno, P.M. Esquivias, J. Navarro, Optimization method for perforated solar screen design to improve daylighting using orthogonal arrays and climate-based daylight modelling, J. Build. Perform. Simul. 10 (2) (2017) 144–160, doi:10.1080/19401493.2016.1197969.
[33] E. Brembilla, Applicability of Climate-Based Daylight Modelling, Loughborough University, 2017 Phd thesis. https://dspace.lboro.ac.uk/2134/28239
[34] L. Bellia, A. Pedace, F. Fragliasso, The role of weather data files in climate-based daylight modeling, Sol. Energy 112 (2015) 169–182, doi:10.1016/j.solener.2014.11.033.
[35] A. Nabil, J. Mardaljevic, Useful daylight illuminance: a new paradigm for assessing daylight in buildings, Light. Res. Technol. 37 (1) (2005) 57–58, doi:10.1191/1365782805li128oa.
[36] J. Mardaljevic, Climate-based daylight modelling and its discontents, in: CIBSE Tech. Symp., 2015, pp. 1–12. April, London
[37] C.F. Reinhart, Daylight Availability and Manual Lighting Control in Office Buildings: Simulation Studies and Analysis of Measurement, University of Karlsruhe, Germany, 2001 Ph.D. thesis.
[38] L. Heschong, Heschong Mahone Group, Daylight Metrics PIER Daylighting Plus Research Program, Technical Report, California Energy Commission, 2011.
[39] S. Subramaniam, Daylighting Simulations with Radiance using Matrix-based Methods, Technical Report, Lawrence Berkeley National Laboratory, 2017.
[40] J. Mardaljevic, Verification of program accuracy for illuminance modelling: assumptions, methodology and an examination of conflicting findings, Light. Res. Technol. 36 (3) (2004) 217–239, doi:10.1191/1477153504li120oa.